Analysis, Modeling, and Simulation of the Phase-Hop Condition in Transformers: The Largest Inrush Currents

Ashkan Farazmand, Francisco de León, *Senior Member, IEEE*, Kuang Zhang, *Student Member, IEEE*, and Saeed Jazebi, *Student Member, IEEE*

***Abstract*—Inrush currents in transformers can have very disruptive effects, such as voltage sags, false tripping of the protective devices, and mechanical stresses in the transformer windings. This paper shows that there are operating situations that may cause a transformer to draw abnormally high inrush currents. Examples include the normal operation of offline uninterruptible power-supply (UPS) systems, interruptions, voltage sags, and notching. These conditions may produce inrush-like currents of more than twice the value of the "normal" maximum inrush caused by energizing at voltage zero-crossing. For this condition, the term "phase-hop" is used in this paper. Laboratory experiments were performed on four different transformers (1 kVA) with varied characteristics and show the impact of phase-hop in the magnitude of inrush currents. The experiments are also used to validate the Electromagnetic Transients Program model used for the analysis of multiple cases. In addition, the behavior of the magnetic flux in a transformer under phase-hop is investigated and compared with different operating conditions using finite elements. The results of this paper have implications in transformer design and in the operation and design of UPS systems to prevent the damaging effects of phase-hop.**

***Index Terms*—Inrush currents, interruptions, phase-hop, transformer modeling, uninterruptible power-supply (UPS) systems, voltage sags.**

I. Introduction

POWER-QUALITY (PQ) problems are critical issues nowadays because of the increased use of power electronics loads. Interruptions and blackouts are the worst forms of power quality problems. Blackout is a complete loss of supply voltage or load current for longer than a minute [1]. Harmonics, interharmonics, power frequency variations, voltage unbalances, interruptions, notching, undervoltages, overvoltages, swells, noise, dc offset, voltage fluctuations, and voltage sags are common power system operation phenomena which cause PQ problems [2].

Manuscript received June 16, 2013; accepted October 08, 2013. Date of publication February 17, 2014; date of current version July 21, 2014. This work was supported by the U.S. Department of Energy under Grant DEOE0000072. Paper no. TPWRD-00680-2013.

The authors are with the Department of Electrical and Computer Engineering, Polytechnic University, Brooklyn, NY 11201 USA (e-mail: farazmand@nyu.edu; fdeleon@poly.edu; kzhang02@students.poly.edu; jazebi@ieee.org).

Color versions of one or more of the figures in this paper are available online at http://ieeexplore.ieee.org.

Digital Object Identifier 10.1109/TPWRD.2013.2286828

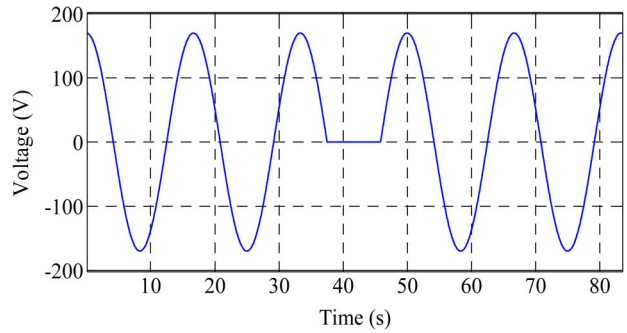

Fig. 1. Voltage wave shape of the phase-hop condition.

In order to solve the aforementioned problems, uninterruptible power supplies (UPSs) are often used [3]. UPS systems are designed to automatically provide emergency electricity to critical loads in case of supply voltage failure. Some UPS systems also regulate or filter the utility power [1].

As it will be explained below, the operation of offline UPS systems, interruptions, voltage sags, and notching in power systems can lead to a condition called "phase-hop" coined for the shape of the voltage wave shown in Fig. 1. When this condition occurs, there are two positive (or negative) semi-cycles applied consecutively to the transformer. The maximum phase-hop current has been reported as an important design parameter by engineers of the leading manufacturers of UPS systems for transformers rated at 25 kVA [4].

Phase-hop causes the transformer core to go into a deep saturation level and draws very large inrush-like currents. Transformers and protections need to be designed to prevent false tripping or damages during phase-hop. The large currents could also damage the UPS systems, or cause problems in the switching operation of the rectifiers, since they may not be designed for these abnormally large currents.

This paper introduces and investigates for the first time the effect of phase-hop on transformers. The study is performed both experimentally and with validated computer simulations. It is found that phase-hop currents can be over twice as large as the "normal" maximum inrush currents caused by switching at zero crossing.

False tripping during phase-hop is more probable than during transformer energization because of the unpredictable timing of this phenomenon. In practice, a common technique used to prevent false tripping of the protective devices during transformer

energization is to add a time delay. However, the occurrence of phase-hop is not predictable and a delay cannot be applied.

The correct estimation of phase-hop currents is important for power system design. Inasmuch as their quantification is vital for UPS operation and design since UPS systems are precisely used to provide backup power, therefore false tripping of vital loads could be disastrous.

II. Effects on Transformer Inrush Currents of Power System Electromagnetic Phenomena

The variation of the rms voltage from its nominal value is described by two parameters: the magnitude of the voltage change and its duration. Power system electromagnetic phenomena are classified in four main groups based on the duration of the disturbance: steady state variations, long duration variations, short duration variations, and transients [2].

This section discusses how interruptions, voltage sags, and notching in power systems can produce a phase-hop voltage to be applied to transformers. In this section, it is assumed that a UPS system is not used to prevent these effects.

A. Interruptions

Interruptions are caused by transients that trigger utility breakers or switches to open. A voltage interruption occurs when the supply voltage decreases to less than 10% of its nominal value in one or more phase conductors. The causes for this phenomenon are: faults, component failure, switching, false breaker tripping, and malfunction of control systems.

Depending on the duration of interruptions, they are classified in three types: momentary (0.5 cycle to 3 s), temporary (3 s to 1 min), and sustained (greater than 1 min) [2]. The first two types are short duration variations and the third is a long duration variation. The duration of the interruption depends on the reclosing capability and speed of the protective device. Note that an interruption of exactly 0.5 cycle produces the phase-hop voltage wave shape illustrated in Fig. 1.

B. Voltage Sags

A voltage sag is a short duration decrease of the voltage between 0.1 and 0.9 p.u. of the nominal voltage at the power frequency for durations of 0.5 cycle to 1 min [2]. The IEC word for this phenomenon is "dip" [5]. Sag durations are divided into three categories: instantaneous (0.5 to 30 cycles), momentary (30 cycles to 3 s), and temporary (3 s to 1 min). The causes for this phenomenon are system faults, switching of large loads, and starting of large motors [2]. Voltage sags cause a partial phase-hop, but currents can be larger than the "normal" inrush.

C. Notching

Notching is a repetitive steady state voltage disturbance lasting less than a half cycle. It represents a phenomenon that is considered both a transient and a harmonic distortion since it occurs continuously and the frequency components related to it are high [2]. It can occur in opposite polarity to the main waveform. In this case, it is subtracted from the normal waveform. In an extreme case, notching may lead to a complete loss of voltage for up to a half cycle [3] corresponding to the phase-hop wave of Fig. 1.

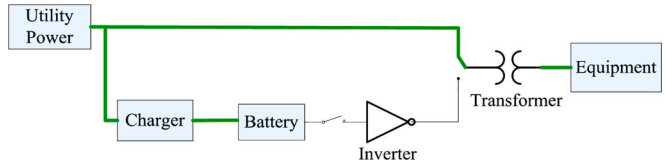

Fig. 2. Off-line UPS performance when utility power is present (normal ac power mode).

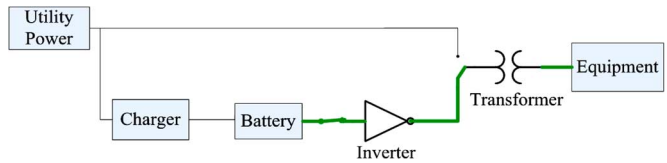

Fig. 3. Offline UPS performance when there is over/undervoltage or power loss (inverter mode).

Notching can be produced during the commutating action from one phase to another in the normal operation of SCR-controlled equipment, such as three-phase converters, motor controls, and inverters. In this condition, a brief short circuit between two phases occurs [3], [6].

III. UPS Systems

UPS systems are intended to provide constant and regulated output voltage and power to critical loads regardless of power quality disturbances present in the mains. The objective is to prevent voltage sags, power outages, impulses, noise, overvoltages or swells, harmonic distortions, frequency variations, voltage fluctuations, and voltage surges [7], [8].

UPSs are classified into two groups: rotary and static. Rotary UPSs normally use a diesel-fueled motor generator set and static UPSs use battery as the backup power source [1]. Because there are several technical problems with rotary UPS systems, most of the modern UPSs are static [1]. There are three kinds of UPSs: offline, line interactive, and online.

A. Offline (Standby) UPS

During the time when the utility power is present, offline UPS systems pass the power directly to the load; the load is not isolated from the mains. During this time, the battery backup is also charged and the inverter connected to the battery is off (see Fig. 2).

When the utility voltage is below a specified value or during a utility power outage, the UPS turns on its internal dc−ac inverter to produce ac power from the battery. In this case, the equipment is connected to the inverter output mechanically (see Fig. 3).

This method saves battery life by avoiding continuous charging and discharging. However, as stated by most manufacturers, there is a switch changeover time between 4 and 10 ms to engage the UPS during an interruption [1]. Practically, this delay can be as long as 25 ms depending on the time that it takes the UPS to detect the absence of utility voltage and transfer to the battery. Therefore, during the changeover time there is a voltage dropout to the connected equipment and the phase-hop condition is possible.

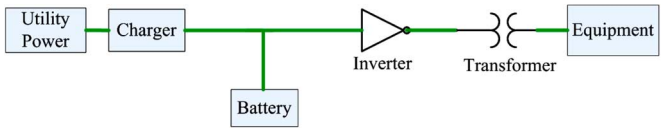

Fig. 4. On-line UPS system.

TABLE I
CIRCUIT PARAMETERS FOR DIFFERENT TRANSFORMERS

Transformer	T_a	T_b	T_c	T_d
Rating [kVA]	1	1	1	1
Rated voltage	120	120	120	120
Turns ratio	1:1	1:1	1:1	1:1
Construction	Shell-type	Shell-type	Toroidal	Toroidal
R_1 [Ω]	0.404	0.251	0.338	0.318
R'_2 [Ω]	0.345	0.324	0.288	0.271
L_s [mH]	0.254	0.692	8.843	0.232
R_{m1} [Ω]	2656	739	2149	2832
R_{m2} [Ω]	2656	739	2149	2832
L_{m1} [mH]	822	753	3339	2569
L_{m2} [mH]	822	753	3339	2569

B. Line-Interactive UPS

Line-interactive UPS is an offline UPS connected with a tap-switching automatic voltage regulator (AVR). In this system, when the power comes from the utility line, the AVR senses the UPS output voltage. When the utility voltage is low (utility brownout), the AVR automatically switches transformer taps to increase the output voltage. When the utility voltage is large, the AVR reduces the output voltage. The setup of this case is the same as the offline UPS (Figs. 2 and 3) with the addition of a multitap variable voltage auto transformer after the utility block. In this case, the load is not completely isolated from the mains power and therefore, phase-hop can occur.

C. Online UPS

The online UPS system, as shown in Fig. 4, converts incoming ac power to rectified and regulated dc voltage and then the inverter regenerates a regulated, clean, and sinusoidal ac power from the dc voltage. Therefore, the load is isolated from the utility. This double conversion system leads to the elimination of line noise, transients, harmonic distortion, and voltage/frequency instability problems from the utility.

In this system, the load is always powered by the inverter and the battery is connected to the dc bus. Therefore, this is a no-break system and there is no change-over time and phase-hop will not occur. This system provides a fully charged battery backup available at all times. It has the disadvantage of shorter battery life because of the continuous charging and discharging of the battery. This UPS system is more expensive and less reliable than standby and line-interactive UPSs because there are additional components connected in series.

IV. TRANSFORMER MODEL

In this paper, the π model is selected to represent the transformer [9]. Tests have been performed on four different transformers (T_a, T_b, T_c, and T_d) to obtain the parameters. Transformer T_a consists of four windings. In this paper, the innermost winding is called the first winding, the one after is called second winding, and so forth. The open-circuit test is used to obtain the magnetizing parameters of the transformers as in [9]. The leakage parameters of the transformers are obtained accurately from the bucking test [10].

TABLE II
AIR-CORE INDUCTANCES FOR THE FOUR TRANSFORMERS UNDER STUDY

Transformer	T_a				T_b	T_c	T_d
Winding	1st	2nd	3rd	4th			
Air-core inductance [μH]	645	850	1,069	1,300	1,000	463	316

The total series ac resistance $R_1 + R'_2$ is computed from

$$R_1 + R'_2 = \frac{P_{BK}}{I_{BK}^2}. \tag{1}$$

Individual breakdown of the resistances is done based on the dc resistance division between primary and secondary dc windings obtained from the dc test. Total leakage inductance is computed from

$$L_s = \frac{1}{2\pi f}\sqrt{\left(\frac{V_{BK}}{I_{BK}}\right)^2 - (R_1 + R'_2)^2} \tag{2}$$

where P_{BK} is the active power computed from the bucking test. V_{BK} and I_{BK}, are the rms values of voltages and currents in the bucking test, respectively. L_s is the total leakage inductance. R_1 and R'_2 are the primary and the secondary ac resistances, respectively, and $f = 60$ Hz. The applied voltage is 125 V rms.

The parameters computed from measurements are shown in Table I. Data given for transformer T_a is for the innermost (first) winding. Hysteresis loops of the three transformers are obtained from Faraday's Law integrating the induced voltage to find the flux as in [9].

The proper estimation of the air-core inductance is highly important to compute the inrush current precisely. 3-D finite-element method (FEM) simulations (using the commercial program Maxwell 14) are carried out. The air-core inductance is calculated as follows [9], [11]:

$$L_{\mathrm{air-core}} = \frac{2W}{I^2} \tag{3}$$

where W is the volume magnetic energy (computed from FEM), and I is the winding current. Table II presents the air-core inductances of the four transformers. The air-core inductances are used to complete the hysteresis loops. They are the slopes used to extend the hysteresis loops from the final measured point (obtained from the open circuit test) to infinity. The model is implemented in the EMTP-RV [12].

V. MODEL VALIDATION AND WORST PHASE-HOP CURRENTS

To validate the model, laboratory experiments are performed on all four transformers under the worst possible phase-hop conditions. In this case, the phase-hop condition occurs following the moment of energizing the transformer using the zero-crossing switch. A zero-crossing and phase-hop switch is built and utilized in the laboratory to connect and disconnect transformers at specific time-instants. For the zero-crossing condition, the switch energizes the transformer when the voltage of the ac power source crosses zero. For phase-hop, the switch, in

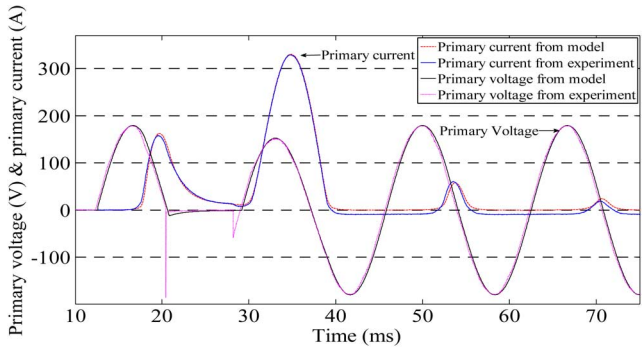

Fig. 5. Comparison of model and experiment for the worst case of phase-hop for the first winding of transformer $\mathrm{T_a}$. One can see a perfect agreement between simulation and experiment.

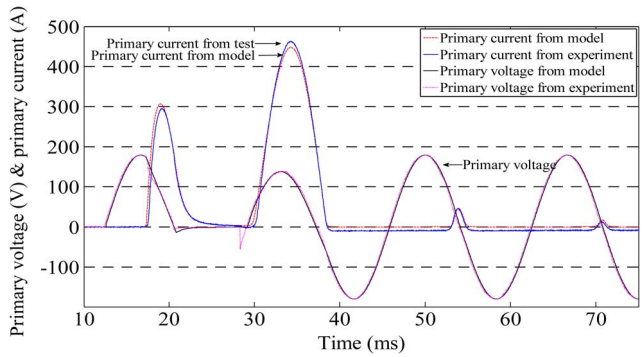

Fig. 6. Comparison of model and experiment for the worst case of phase–hop for transformer $\mathrm{T_d}$. One can see a very good match between simulation and experiment.

addition to energizing the transformer at voltage zero-crossing, opens the connection between the second and third zero-crossings, thus re-establishing power at the third zero-crossing (see Appendix for more details).

Fig. 5 shows the waveshapes and compares the results from experiments and the model for the first winding of transformer $\mathrm{T_a}$. The first peak values of inrush current (caused by the first peak of the primary voltage) from experiment and simulation are 157.7 A and 162.5 A, respectively (difference of 3%). The second peak (caused by the phase-hop voltage) from experiment and simulation are 328.9 A and 330.2 A, respectively (difference of only 0.4%). Fig. 6 compares the results for transformer $\mathrm{T_d}$ under the abovementioned condition. The difference between the peak currents of the model and the experiment is 3.9% for the first peak and 3.3% for the second peak. Note, however, that the inrush and phase-hop currents are much higher because transformer $\mathrm{T_d}$ is a toroidal transformer.

Tables III and IV compare the results of the first and second peaks of inrush current under the worst case of phase-hop for all four transformers under study. Looking at Figs. 5 and 6 and Tables III and IV, one can observe a strong agreement between simulation and experimental results.

Note from Figs. 5 and 6 that the second positive peak of the voltage in the phase-hop condition is smaller than the first peak. The reason for this is the existence of a large voltage drop in the source resistance ($R_{\mathrm{source}} = 0.1\ \Omega$) caused by the extremely large phase-hop currents. If the short-circuit power rating of the source was larger, higher inrush (and phase-hop) currents would occur.

TABLE III
FIRST PEAK VALUES OF INRUSH CURRENT FOR DIFFERENT TRANSFORMERS UNDER WORST CASE OF PHASE-HOP (EXPERIMENT VERSUS SIMULATION)

Transformer	Winding	Test [A]	Model [A]	Difference [%]
$\mathrm{T_a}$	1st	157.7	162.5	3.0
	2nd	130.4	134.5	3.1
	3rd	125.2	122.3	-2.4
	4th	123.1	111.1	-9.7
$\mathrm{T_b}$		149.9	153.1	2.1
$\mathrm{T_c}$		208	213.2	2.5
$\mathrm{T_d}$		295.4	307	3.9

TABLE IV
SECOND PEAK VALUES OF INRUSH CURRENT FOR DIFFERENT TRANSFORMERS UNDER WORST CASE OF PHASE-HOP (EXPERIMENT VERSUS SIMULATION)

Transformer	Winding	Test [A]	Model [A]	Difference [%]
$\mathrm{T_a}$	1st	328.9	330.2	0.4
	2nd	291.3	272.4	-6.5
	3rd	261.7	252.5	-3.5
	4th	240.5	238.4	-0.9
$\mathrm{T_b}$		353.3	368.5	4.3
$\mathrm{T_c}$		402.3	360.9	-10.3
$\mathrm{T_d}$		463.3	447.9	-3.3

VI. TRANSFORMERS UNDER THE PHASE-HOP CONDITION

In practice, it may not be common to have the phase-hop condition right after the transformer energization (inrush). That circumstance was used in Section IV to analyze this extreme, yet possible, case of phase-hop and validate the model. The most practical and probable condition of the phase-hop is when it happens during the normal operation in steady state (long after energizing the transformer for the first time). In order to simulate this condition in the EMTP and compare the results, the transformer is energized at voltage zero-crossing and after reaching the steady state, phase-hop occurs.

The results for the first winding of transformer $\mathrm{T_a}$ under phase-hop are shown in Fig. 7(a). The first peak of inrush current is 162.5 A while the one caused by phase-hop is 313.3 A. Fig. 7(b) shows a closer view of the phase-hop condition for this case. Fig. 8(a) and 8(b) presents the results for transformer $\mathrm{T_d}$ under typical phase-hop condition. The first peak of inrush current is 307 A, and the second peak is 1.46 times higher at 446.8 A. Table V compares the results for all four transformers for the inrush currents caused by zero-crossing voltage, typical condition of phase-hop, and worst case of phase-hop through simulation. One can appreciate that the values of inrush current from the phase-hop condition are much higher than the first peak of inrush current caused by zero-crossing voltage. As an example, for transformer $\mathrm{T_b}$, the peak value of inrush current under normal phase-hop condition is 2.15 times higher than the first peak of inrush current, and under the worst case of phase-hop, it is 2.41 times higher.

Note that for transformers $\mathrm{T_c}$ and $\mathrm{T_d}$, which are toroidal transformers, the difference between peak values of inrush current in the normal and the worst cases of phase-hop is small (see

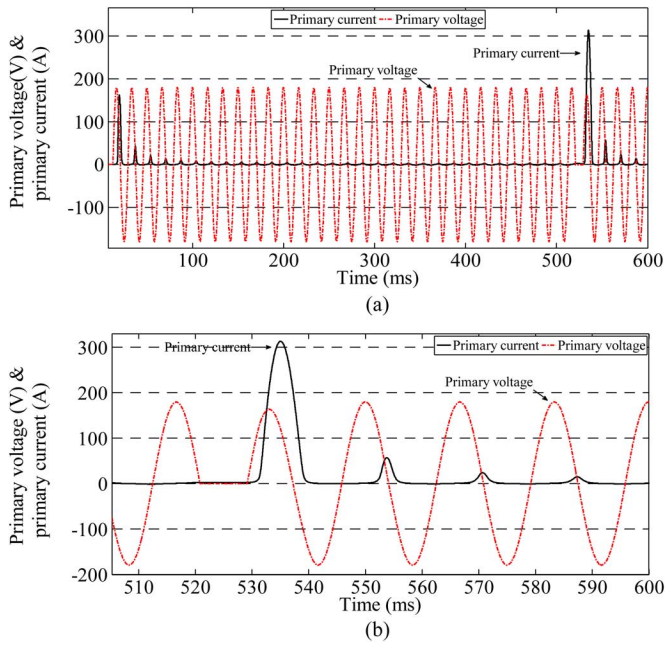

Fig. 7. Simulation of transformer Ta (first winding) under the phase-hop condition. (a) Transient from the beginning of excitation. (b) Close view of the phase-hop part.

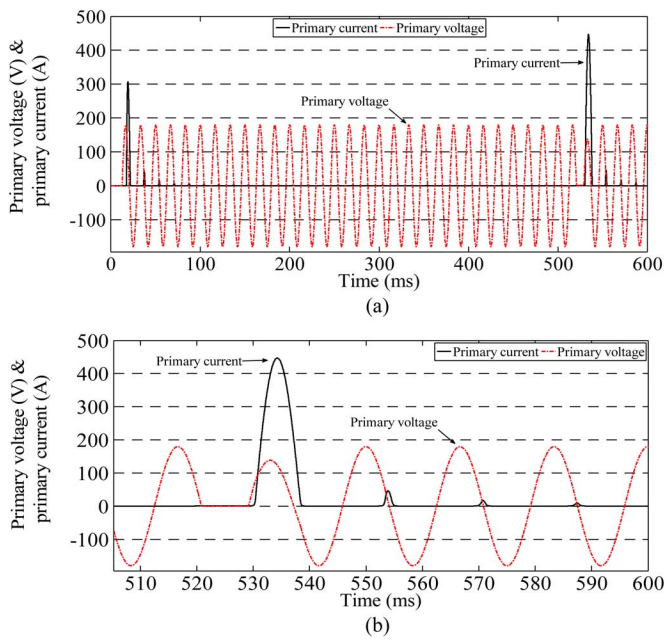

Fig. 8. Simulation of transformer $\mathrm{T_d}$ under phase-hop condition. (a) Transient from the beginning of excitation. (b) Close view of the phase-hop part.

Table V). This is because in these transformers, the hysteresis cycles are thinner and flatter than the ones of standard transformers, because the cores have no gap. Therefore, under the worst case of phase-hop, the first spike of inrush current reached zero at the start of the second peak, while for standard transformers ($\mathrm{T_a}$ and $\mathrm{T_b}$), the second inrush current occurs while the current is not yet zero; see Figs. 5 and 6 to compare the results for transformers $\mathrm{T_a}$ and $\mathrm{T_d}$.

TABLE V
COMPARISON OF MAXIMUM INRUSH CURRENT UNDER DIFFERENT CONDITIONS FOR DIFFERENT TRANSFORMERS

Transformer	Winding	First Peak (inrush) [A]	Second Peak (phase-hop) [A]	Second Peak (worst case) [A]
$\mathrm{T_a}$	1st	162.5	313.3	330.2
	2nd	134.5	257.6	272.4
	3rd	122.3	237.4	252.5
	4th	111.1	222.0	238.4
$\mathrm{T_b}$		153.1	329.8	368.5
$\mathrm{T_c}$		213.2	359.3	360.9
$\mathrm{T_d}$		307	446.8	447.9

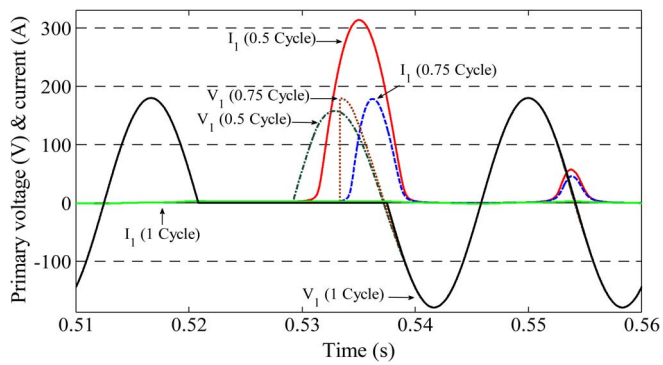

Fig. 9. Primary voltage and caused inrush current of the first winding of the transformer Ta under 0% interruption.

Fig. 9 shows the effect of the duration of an interruption on phase-hop current. The primary currents and the applied voltage (primary voltage) to the first winding of the transformer $\mathrm{T_a}$ are presented for a zero volts interruption lasting 0.5, 0.75, and 1 cycle. One can see that the largest peak current is when the duration of the interruption is half a cycle (313.3 A), which is almost twice the normal zero-crossing inrush current (162.5 A). Under this situation, a complete instance of phase-hop occurs. The case with no inrush current is when the duration of the interruption is one full cycle. This situation corresponds to the normal sinusoidal condition since one complete cycle is eliminated. For an interruption of 0.75 cycle, the peak current is 178.1 A.

An example of a voltage sag is presented in Fig. 10. The primary voltage and inrush currents under zero-crossing and 10% voltage sag lasting for 10.5 cycle are shown, for the first winding of transformer $\mathrm{T_a}$. The value of inrush current caused by the sag is 274.7 A (69% larger than the zero-crossing inrush current).

Table VI summarizes the inrush current results for 0% and 5% interruptions, and for 10% and 50% voltage sags. The duration of the transient is between half a cycle (worst case) and 3600.5 cycles (around 1 min). As shown in Table VI, the worst cases of inrush-like currents occur when the fault duration is $0.5 + n$ cycles; where $n = 0, 1, 2 \ldots$. This is so because there are two half cycles consecutively, which is the complete phase-hop. In contrast, for sags lasting $0.5+n$ cycles, there is a small flux-cancellation effect which decreases magnitude of the inrush current. To illustrate this, the 20% sag with 2.5-cycle duration ($n = 2$) is depicted in Fig. 11. Note that the integral of the voltage is the flux. The areas A, B, C, and D cancel each other but the extra half cycle, E (highlighted in Fig. 11) leads to a decrease in the

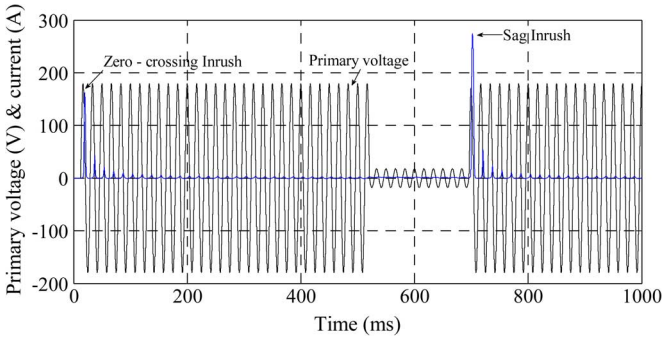

Fig. 10. Primary voltage and caused inrush current of the first winding of the transformer Ta under 10% voltage sag for 10.5-cycle duration.

TABLE VI
INRUSH CURRENTS UNDER DIFFERENT KINDS OF INTERRUPTIONS AND VOLTAGE SAGS FOR THE FIRST WINDING OF TRANSFORMER T_a

	Current Peak Value (A)			
	interruption	interruption	sag	sag
# of cycles	0%	5%	10%	50%
0.5	313.3	305.3	296.1	182
0.6	296.4	287.4	277.4	162.9
0.7	232.3	222.7	212.3	105.3
0.8	109.1	101.7	93.6	20.8
0.9	5.11	5	4.85	3.6
1	2.2	2.3	2.3	2.4
1.1	4.9	4.79	4.6	3.5
1.5	310.7	302.7	293.5	179.5
2.5	308.3	300.2	291	177.1
10.5	293	283.93	274.7	160.5
100.5	228.4	213.82	199.7	73.81
3600.5	201.5	184.3	166.9	37

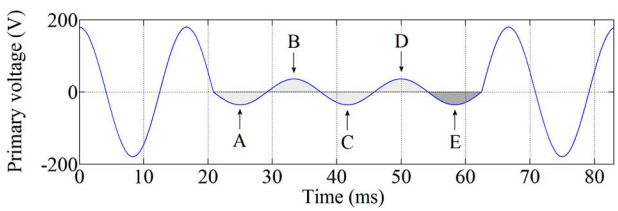

Fig. 11. The 20% sag with 2.5-cycle duration.

built flux. This is the reason why sags with larger voltage magnitude, cause smaller inrush currents.

In addition, a longer interruption or voltage sag causes a larger reduction in the built flux and as a result in the inrush currents (see Table VI).

To complete the study, EMTP simulations for various undervoltages were performed [2], [3]. Undervoltages lasting longer than 1 min with magnitudes between 0.8 and 0.9 p.u. were analyzed. In no case, including undervoltages lasting $0.5+n$ cycles, the phase-hop phenomenon is observed.

Form this study, it is concluded that under the phase-hop condition a very large current can be drawn by transformers due to heavy saturation of the iron core. Therefore, phase-hop should be considered in transformer and UPS design and operation to prevent its potential destructive effects. As it was shown, phase-hop can occur partially or fully depending on the magnitude and duration of electromagnetic phenomena causing distorted input voltage to the transformer.

VII. PHYSICAL EXPLANATION OF THE PHASE-HOP CONDITION

Figs. 12 and 13 explain the phase-hop phenomenon physically by illustrating the behavior of the primary voltage, internal voltage, magnetic flux, and current. The graphs correspond to the first winding of the transformer T_a under the worst condition of phase-hop (phase-hop following transformer energization at zero crossing). An important component of the explanation is the internal voltage (E_1), which is computed as follows:

$$E_1 = V_1 - R_1 I_1 \tag{4}$$

where V_1 is the primary terminal voltage, I_1 is the primary current, and R_1 is the primary winding ac resistance.

Nine points: a, b, c, d, e, f, g, h, and i are identified in Figs. 12 and 13 to highlight important performance stages of the transformer at different times during the inrush followed by a phase-hop transient.

The energization is done with zero residual flux (point a). At that instant, voltage, current, and flux are all zero. When the voltage reaches its first peak (at point b) a quarter of a cycle later, magnetic flux is building (0.4 Wb) and the current is still small at about the value of the normal magnetizing current, 0.6 A peak. At point c, the internal voltage is crossing zero from positive to negative, at that moment the magnetic flux presents a first peak (0.81 Wb) and the "normal" peak of the inrush currents is reached (162.5 A). Then, the phase-hop occurs and the negative semi-cycle of the voltage, between points c and d disappears [see Fig. 13(a) and (b)]. When the terminal voltage reaches the next zero crossing at point d, the flux has reduced a small amount, but it is still at a very high value (0.65 Wb) and the current has not reduced to zero (11.8 A). Because of the existence of a positive voltage between points d and e, the flux increases further until the transient reaches the maximum at point e with a flux of 0.95 Wb and a phase-hop current of 330.2 A, which is almost twice as large as the zero-crossing inrush current. At this time, the internal voltage is crossing zero from positive to negative. From this point on, the peaks of magnetic flux and current reduce in magnitude as the dc component damps. At point f voltage reaches its first negative peak after phase-hop, with the value of 0.3 Wb for the flux and 0.31 A for the primary current. The reversing points of the hysteresis cycle in the third quadrant (points g, h and i) progressively decrease as the transient damps out and the flux becomes increasingly symmetric. The magnitudes of the magnetic flux are -0.2 Wb, -0.26 Wb, and -0.28 Wb for these three points, respectively, which correspond to the voltage zero crossings from negative to positive.

VIII. MAGNETIC-FIELD BEHAVIOR

To shed light into the internal behavior of the transformer, in this section, the magnetic field of the transformer is investigated for different operating conditions including: open circuit, normal operation (on-load), zero-crossing inrush, and phase-hop. Simulations are performed using the FEM computer program, Maxwell 14. Magnetic flux lines are shown inside and outside the core in Fig. 14. Note that due to the geometrical symmetry of the transformer, only a part of the core is shown.

During open circuit for the situation presented in Fig. 14(a), the magnetic field is concentrated inside the iron core (the lines

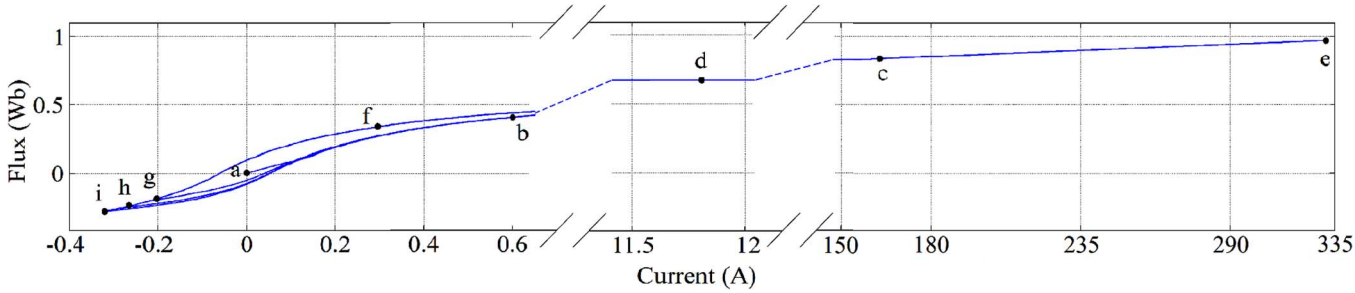

Fig. 12. Core flux versus primary current for the first winding of transformer Ta under the worst condition of phase-hop.

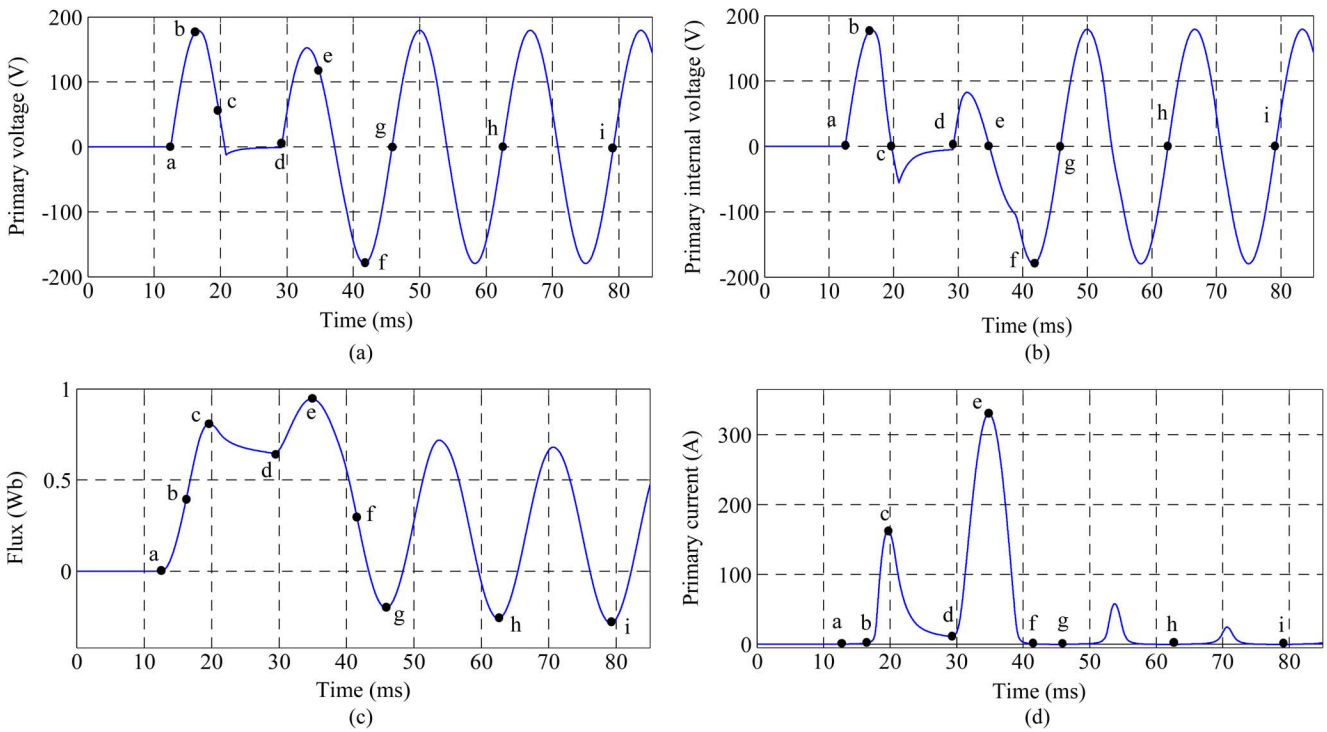

Fig. 13. (a) Primary voltage versus time. (b) Primary internal voltage versus time. (c) Core flux versus time. (d) Primary current versus time for the first winding of the transformer T_a under the worst condition of phase-hop.

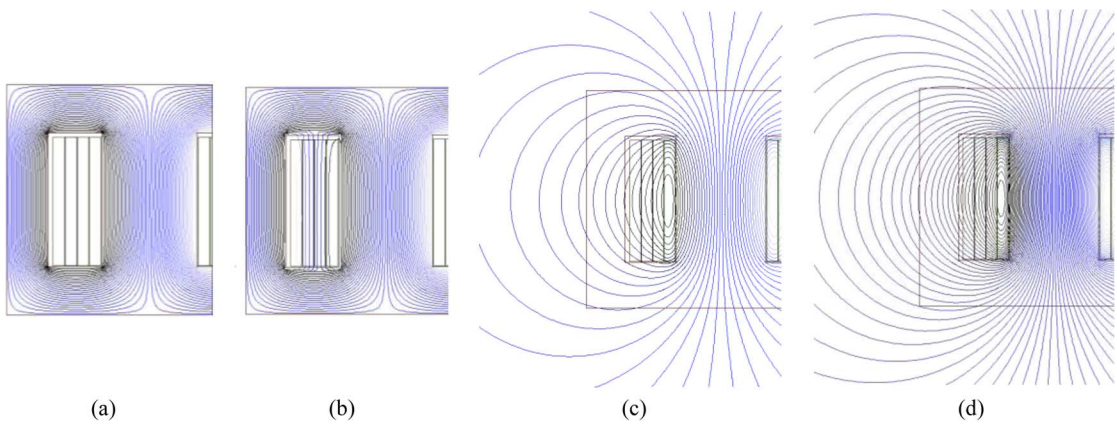

Fig. 14. Magnetic field behavior for the saturated and nonsaturated transformer iron core: (a) open circuit, (b) normal operating condition—transformer loaded, (c) peak condition for inrush currents at zero-crossing switching, and (d) peak condition for phase-hop currents.

in the window are the boundaries of the windings). During normal operation, when the transformer is supplying the nominal load, a part of magnetic flux "leaks" into the interwinding region [see Fig. 14(b)]. This flux is what produces the leakage inductance. In Fig. 14(c), the magnetic flux for transformer energization at zero crossing is presented. One can see that there is a considerable amount of flux in the air. In fact, the flux distribution resembles the behavior of an air-core inductor. As shown in Fig. 14(d), the flux pattern during the phase-hop does not change significantly in comparison with that of the

normal inrush current. However, the amplitude (seen by the concentration of lines) of the magnetic field is larger.

IX. Possible Solutions for Phase-Hop

The transient phenomenon known as transformer inrush currents was first published by John Fleming in 1892 [13]. Since then, many publications have proposed techniques to limit inrush currents to prevent its destructive effects. Some of the methods are external (to the transformer) and others are transformer-based solutions. External solutions consist of preinsertion impedances, negative temperature coefficient thermistors (NTC) [14], transformer core demagnetizing [15], phase-delayed switching [16], [17], and sequential phase energization [18], [19]. Transformer-based solutions consist of air gaps, virtual gaps [20], using low permeability materials for the core, and special designs with larger values of air-core inductance.

To some extent, each of the existing approaches diminishes inrush currents; however, there is a trade-off with each one of them. In addition, some methods are not applicable for phase-hop. External demagnetizing techniques, for example, are not possible because there is not enough time to demagnetize the transformer core during the half a cycle between two consecutive peaks. Switching methods have some problems with the mutual effects with switches applied in the UPS systems and also the reliability of the system. Implementations of preinsertion impedance methods are very complicated due to the difficulty in the detection of the phase-hop condition. Thermistors do not work either because at the time of the phase-hop the system is already on, therefore, thermistor resistances are very small and cannot reduce the inrush current effectively. In general, there are several problems with the addition of series components with the transformer: (1) the reliability of the system reduces, and (2) depending on the voltage level the additional components need to comply with safety standards, which makes them expensive.

It seems that the best solutions to prevent the destructive effects of the phase-hop phenomena are transformer based. Application of these methods will be treated in a forthcoming paper.

X. Conclusion

This paper has shown, for the first time, how the occurrence of the phase-hop phenomenon in transformers can lead to extremely large currents. Phase-hop can occur at any time in a power system because interruptions, voltage sags, and notching in the network are not predictable. In order to prevent these phenomena, a UPS system can be used. However, the action of offline UPS systems may itself lead to large levels of inrush currents for the transformers located between the load and the UPS system as well.

The value of the phase-hop currents can be several times higher than the magnitude of the "normal" inrush currents that occur when a transformer is energized at voltage zero-crossing.

The extremely large currents produced by the phase-hop condition can lead to serious problems, such as PQ issues, mechanical stresses on transformer windings, and false tripping of vital protections. The best techniques to prevent these serious effects seem to be transformer-based solutions.

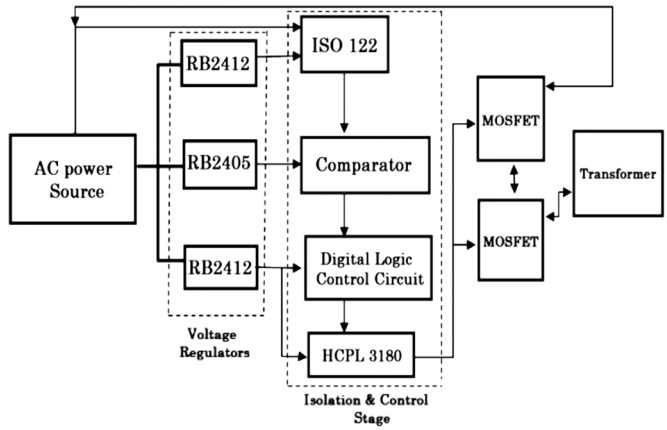

Fig. 15. Power and control circuits implemented in the zero-crossing and phase-hop switch.

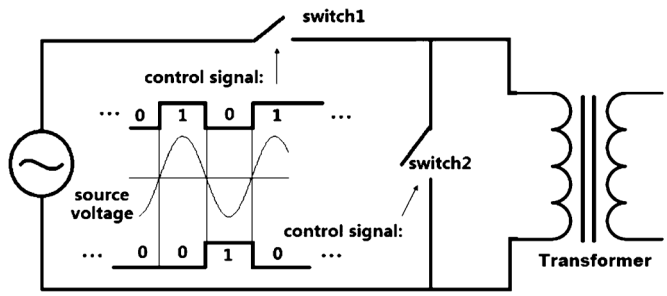

Fig. 16. Schematics of the phase-hop circuit.

Appendix

Fig. 15 presents a block diagram of the power and control circuits implemented in the zero-crossing and phase-hop switch developed for this project. This switch consists of voltage regulators, optoisolators, a digital logic control circuit, and metal–oxide semiconductor field-effect transistor (MOSFET) switches. When the ac power source is on, the optoisolator will pass the sinusoidal waveform to a comparator, which checks for a zero value. As a result, a 50% duty ratio square wave, which rising and falling edges correspond to the zero-crossing of power source, appears at the output of comparator. The first rising edge triggers the digital logic control circuit, which turns on the switch and finally energizes the transformer.

The phase-hop circuit of the switch is essentially the same as the zero-crossing circuit except for the digital logic control circuit and an extra pair of MOSFETs. Three precise timers are utilized in the control circuit to generate the signals for switches 1 and 2 in Fig. 16. Switch 1 consists of two MOSFETs. It closes at the first zero-crossing and only opens between the second and third zero-crossings. Switch 2 is added to prevent cutting large inductive currents. When switch 2 is closed, the inrush current inside the transformer will only flow through switch 2. As a result, switch 1 and other circuit elements are protected from the high voltages caused by large di/dt values.

Acknowledgment

The authors would like to thank N. Mahamedau, ex-student of Polytechnic Institute of New York University, for his collab-

oration in building the phase-hop switch and performing the experiments during this project.

REFERENCES

[1] B. W. Kennedy, *Power Quality Primer*. New York: McGraw-Hill, 2000, pp. 122–125.

[2] *IEEE Recommended Practice for Monitoring Electric Power Quality*, IEEE Standard 1159-1995, Jun. 1995.

[3] *IEEE Recommended Practice for Powering and Grounding Electronic Equipment*, IEEE Standard 1100-1999, Mar. 1999.

[4] Private communications between engineers of American Power Conversion and Liebert with the second author. Toronto, ON, Canada, 1999.

[5] *Electromagnetic Compatibility (EMC): Testing and Measurement Techniques-Voltage Dips, Short Interruptions and Voltage Variations Immunity Tests*, IEC Standard 61000-4-11, Mar. 2004.

[6] *IEEE Recommended Practice and Requirements for Harmonic Control in Electrical Power Systems*, IEEE Standard 519-1992, Apr. 1993.

[7] J. M. Guerrero, L. G. de Vicuna, and J. Uceda, "Uninterruptible power supply systems provide protection," *IEEE Ind. Electron. Mag.*, vol. 1, no. 1, pp. 28–38, Spring, 2007.

[8] J. Seymour, "The seven types of power problems," white paper 18, Revision1, Schneider Electric—Data Center, Science Center, 2011. [Online]. Available: http://www.apc.com/prod_docs/results.cfm?DocType=White%20Paper&Query_Type=3&Value=21

[9] F. de León, A. Farazmand, and P. Joseph, "Comparing the T and pi equivalent circuits for the calculation of transformer inrush currents," *IEEE Trans. Power Del.*, vol. 27, no. 4, pp. 2390–2398, Oct. 2012.

[10] F. de León and A. Semlyen, "Efficient calculation of elementary parameters of transformers," *IEEE Trans. Power Del.*, vol. 7, no. 1, pp. 376–383, Jan. 1992.

[11] F. de León, S. Jazebi, and A. Farazmand, "Accurate measurement of the air-core inductance of iron-core transformers with a non-ideal low power rectifier," *IEEE Trans. Power Del.*, accepted for publication.

[12] J. Mahseredjian, S. Dennetière, L. Dubé, B. Khodabakhchian, and L. Gérin-Lajoie, "On a new approach for the simulation of transients in power systems," *Elect. Power Syst. Res.*, vol. 77, no. 11, pp. 1514–1520, Sep. 2007.

[13] J. A. Fleming, "Experimental researches on alternate-current transformers," *J. Inst. Elect. Eng.*, vol. 21, no. 101, pp. 594–686, Nov. 1892.

[14] K. Billings and T. Morey, *Switchmode Power Supply Handbook*, 2nd ed. New York: McGraw Hill, 1989, pp. 1–6.

[15] B. Kovan, F. de León, D. Czarkowski, Z. Zabar, and L. Birenbaum, "Mitigation of inrush currents in network transformers by reducing the residual flux with an ultra-low-frequency power source," *IEEE Trans. Power Del.*, vol. 26, no. 3, pp. 1563–1570, Jul. 2011.

[16] J. H. Brunke K. J. Frohlich, "Elimination of transformer inrush currents by controlled switching. I. Theoretical considerations," *IEEE Trans. Power Del.*, vol. 16, no. 2, pp. 276–280, Apr. 2001.

[17] J. H. Brunke and K. J. Frohlich, "Elimination of transformer inrush currents by controlled switching. II. Application and performance considerations," *IEEE Trans. Power Del.*, vol. 16, no. 2, pp. 281–285, Apr. 2001.

[18] Y. Cui, S. G. Abdulsalam, S. Chen, and W. Xu, "A sequential phase energization technique for transformer inrush current reduction—Part I: Simulation and experimental results," *IEEE Trans. Power Del.*, vol. 20, no. 2, pt. 1, pp. 943–949, Apr. 2005.

[19] W. Xu, S. G. Abdulsalam, Y. Cui, and X. Liu, "A sequential phase energization technique for transformer inrush current reduction—Part II: Theoretical analysis and design guide," *IEEE Trans. Power Del.*, vol. 20, no. 2, pt. 1, pp. 950–957, Apr. 2005.

[20] V. Molcrette, J. L. Kotny, J. P. Swan, and J. F. Brudny, "Reduction of inrush current in single-phase transformer using virtual air gap technique," *IEEE Trans. Magn.*, vol. 34, no. 4, pp. 1192–1194, Jul. 1998.

Ashkan Farazmand was born in Tehran, Iran, in 1983. He received the M.Sc. (Hons.) degree in electrical engineering from the University of Tehran, Tehran, Iran, in 2009, and the Ph.D. degree (Hons.) in electrical engineering from the Polytechnic Institute of New York University, Brooklyn, NY, USA, in 2013.

Currently, he is a Postdoctoral Fellow in the Electrical and Computer Engineering Department, Polytechnic Institute of New York University. His research interests are the design and analysis of transformers, electrical transients, derating of electrical machines under nonsinusoidal and unbalanced conditions, and power quality.

Francisco de León (S'86–M'92–SM'02) received the B.Sc. and the M.Sc. (Hons.) degrees in electrical engineering from the National Polytechnic Institute, Mexico City, Mexico, in 1983 and 1986, respectively, and the Ph.D. degree in electrical engineering from the University of Toronto, Toronto, ON, Canada, in 1992.

He has held several academic positions in Mexico and has worked for the Canadian electric industry. Currently, he is an Associate Professor at Polytechnic Institute of NYU, Brooklyn, NY, USA. His research interests include the analysis of power phenomena under nonsinusoidal conditions, the transient and steady-state analyses of power systems, the thermal rating of cables and transformers, and the calculation of electromagnetic fields applied to machine design and modeling.

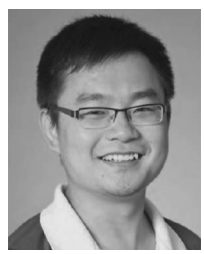

Kuang Zhang (S'12) was born in Ziyang, China, in 1990. He received the B.Eng. degree in electronic engineering from South China University of Technology, Guangzhou, China, in 2013, the B.Sc. degree in electrical engineering from the Polytechnic Institute of New York University, Brooklyn, NY, USA, in 2013, where he is currently pursuing the Ph.D. degree in electrical engineering.

His research interests include modeling, computation, and measurement of transformer inrush currents. He is currently working in the areas of power electronics and power quality.

Saeed Jazebi (S'10) was born in Kerman, Iran, in 1983. He received the B.Sc. degree in electrical engineering from Shahid Bahonar University, Kerman, Iran, in 2006, the M.Sc. degree in electrical engineering from Amirkabir University of Technology, Tehran, Iran, in 2008, and is currently pursuing the Ph.D. degree in electrical engineering at the Polytechnic Institute of New York University, Brooklyn, NY, USA.

His field of interest includes electromagnetic design, modeling, and simulation of electrical machines and power system components, statistical pattern recognition applications in power engineering, power system protection, and power quality.